Supporting Information (SI)

Benzo−crown ether electrolyte additives in facilitating sulfur evolution and lithium anode stabilization for high−performance lithium−sulfur batteries

Zhihua Wang,‡[a] Zhenjun Xue,‡[b] Junru Ke,[a] Min Dong,[a] Bei Ma,[a] Zhe Zhang,[a] Hua Ji,*[cd] Qingmin Ji,[a] He Zhu *[a] and Si Lan *[a]

[a] Herbert Gleiter Institute of Nanoscience, School of Materials Science and Engineering, Nanjing University of Science and Technology, Nanjing, 210094, China. Email: hezhu@njust.edu.cn, lansi@njust.edu.cn

[b] School of Chemistry and Chemical Engineering, Nanjing University, Nanjing, 210023, China

[c] Scientific Research and Innovation Center，Suzhou Nuclear Power Research Institute, Suzhou 215004, China.

[d] National Engineering Research Center for Nuclear Power Plant Safety & Reliability, Suzhou 215004，China.

‡ These authors contributed equally to this work.

Experimental Procedures

Material preparation

Raw materials: All raw materials, including elemental sulfur (S), lithium sulfide (Li_2S), Dibenzo−24−crown−8 (D24C8), polypropylene/polyethylene (PP/PE) Separator, poly (vinylidene fluoride) (PVDF), Super-P (SP), N-methyl pyrrolidone (NMP), aluminum (Al) foil, lithium (Li) foil, 1,3-dioxane (DOL), 1,2-diamethoxyethane (DME), lithium nitrate ($LiNO_3$), lithium bis(trifluoromethanesulfonic)imide (LiTFSI), and carbon cloth (CC) were all purchased from commercial sources. The lithium-sulfur (Li-S) electrolyte consists of 1 M LiTFSI and 1% $LiNO_3$ dissolved in DOL/DME (v/v = 1:1) solvent.

Material preparation for characterization: A solvent-free DOL/DME solution was prepared. The Li_2S_6 solution was prepared by mixing S and Li_2S with a molar ratio of 5:1 in DOL/DME (v/v = 1:1) mixed solvent, followed by vigorous magnetic stirring at 60 ^oC for 24 h under an argon atmosphere. As a result, the brownish-red Li_2S_6 solution (100 mmol L^{-1}) was obtained. Different quantitative amounts of D24C8 powder were dissolved in DOL/DME solution and Li-S electrolytes to obtain a D24C8 solution (100 mmol L^{-1}) and the 4 electrolytes with D24C8 (25, 50, 75, 100 and 125 mmol L^{-1}). Finally, a quantitative amount of D24C8 powder was dissolved in Li_2S_6 solution and electrolyte with 100 mM Li_2S_6 to obtain a D24C8+Li_2S_6 solution (100 mmol L^{-1}) and an electrolyte with D24C8+Li_2S_6 (100 mmol L^{-1}).

Cathode preparation: SP and S were mixed with a weight ratio of 1:3. The mixture was uniformly ground in a mortar for about one hour, and then transferred to a glass tube for sealing. Afterward, the mixture was heated (155 ^{o}C) in a tube furnace (nitrogen atmosphere) for 8 h to obtain SP@S composite material. SP@S (80 wt.%) SP (10 wt.%) and PVDF (10 wt.%) were thoroughly mixed in NMP to form a slurry. The obtained slurry was evenly coated on a piece of carbon-covered Al foil, and vacuum dried at 60 ^{o}C for 8 h. Electrodes with a diameter of 12 mm were cut out by the MSK-T10 manual slicer. The areal sulfur loading of ordinary batteries was controlled at 1.2 mg cm^{-2}.

Materials characterization

^{13}C and ^{7}Li nuclear magnetic resonance (NMR) spectra were recorded on a JNM-ECZ spectrometer with deuterated chloroform as solvent to verify the molecular structure of D24C8. We performed the scanning electron microscopy (SEM) and atomic force microscopy (AFM) tests on the anodes.

Electrochemical characterization

Equipment: The Li-S batteries were tested with a voltage ranging from 1.7 to 2.8 V. Cyclic voltammetry (CV) tests were conducted by a CHI660D electrochemical workstation of Shanghai Chenhua Company. The charge/discharge tests of batteries were performed using the NEWARE Battery Test System (CT-4008Tn-5V10mA-164, Shenzhen, China).

Battery measurements: Coin cells were assembled in a dry and inert glove box with Li foil as the anodes, PP/PE as the separators, electrolytes (the electrolyte content on both sides of the separator was 25 μL) and the cathodes. With D24C8 concentrations of 0, 100 mM in the cathode-side electrolytes, we performed current rate (0.1, 0.2, 0.5, 1, and 2 C), 0.2 and 2 C cycling tests were delivered (1 C = 1672 mA g^{-1}).

Ion diffusion coefficient tests: Using the measured CV data, the peak currents of the four redox peaks were identified respectively, and the Li^+ diffusion coefficient was calculated using the Randles-Sevcik equation as follows:

$$I_p = 2.69 \times 10^5 n^{1.5} A D^{0.5} C v^{0.5}$$

where I_p is the peak current (mA), A is the electrode area (cm^2, in this case 1.13 cm^2), C is the Li^+ concentration (mol cm^{-3}), and v is the scan rate (mV s^{-1}, in this case 0.1-0.5 V s^{-1}), D is the diffusion coefficient (cm^2 s^{-1}), and n is the number of transferred electrons.

Symmetric Li_2S_6 battery measurements: We chose the commercial CC as the current collector, which was cut into circles with a diameter of 12 mm. Two current collectors were assembled into a standard 2032-coin cell with a 20 mm diameter separator, and 48 μL of electrolyte was dropped on each side. Electrolyte types include blank, Li_2S_6 and D24C8+Li_2S_6 electrolytes. CV measurements were carried out at the scan rate of 3 mV s^{-1} in the potential range of −0.8 and 0.8 V.

Deposition of Li_2S: We used Li foil as the negative electrode, porous PP/PE as the separator, CC as the positive current collector and different types of electrolytes (the positive and negative electrodes were Li_2S_6/D24C8+Li_2S_6 electrolytes and ordinary Li-S electrolyte, respectively) to assemble the batteries. The batteries were galvanostatically discharged to 2.08 V at 0.112 mA, and then potentiostatic discharged at 2.07 V to promote Li_2S nucleation and growth until the current was below 0.01 mA.

Li^+ transference number: The Li^+ transference number (t_{Li+}) was obtained by the symmetric Li−Li batteries via EIS and chronoamperometry measurements, and t_{Li+} was calculated using the Bruce−Vincent−Evans equation:

$$t_{Li+} = \frac{I_{ss}(\Delta V - I_0 R_0)}{I_0(\Delta V - I_{SS} R_{SS})}$$

where ΔV is the applied polarization voltage (10 mV) across the cell, R_0 and R_{ss} represent the interfacial resistances before and after polarization, respectively, I_0 and I_{ss} are the initial current before the polarization and the stable current after the polarization, respectively.

Theoretical simulation

All calculations were carried out with the Gaussian 16 A 03 software. The B3LYP functional was adopted for all calculations in combination with the Grimmer's D3(BJ) dispersion correction. For geometry optimization and frequency calculations, the def2-

SVP basis set was used for all atoms. The singlet point energy calculations were performed with a larger basis set def2-TZVP. The polarizable continuum model (PCM) implicit solvation model was used to account for the DOL/DME solvation effect when performing single point energy calculations. The static dielectric constant parameter of the solvent was set to 7.1 according to the mixture volume ratio (1:1) of the solvent. All wave function analyses (electrostatic potential, molecular surface quantitative analysis, electron density difference, and so on) as well as a drawing of various kinds of maps were finished via the Multiwfn code. Some isosurface maps were rendered by means of the VMD visualization program based on the files exported by Multiwfn.

Supplementary Figures

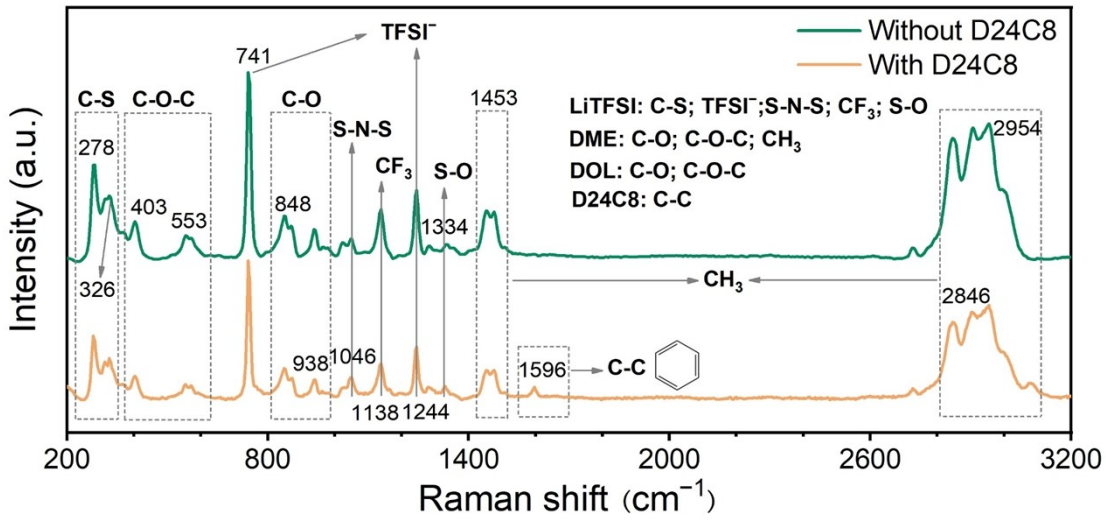

Figure S1. Raman spectra of electrolyte with and without D24C8.

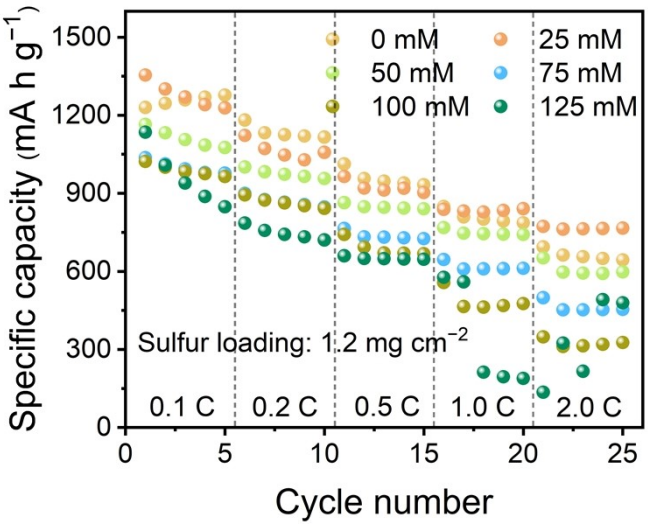

Figure S2. Rate performance of Li-S batteries with different concentrations of D24C8.

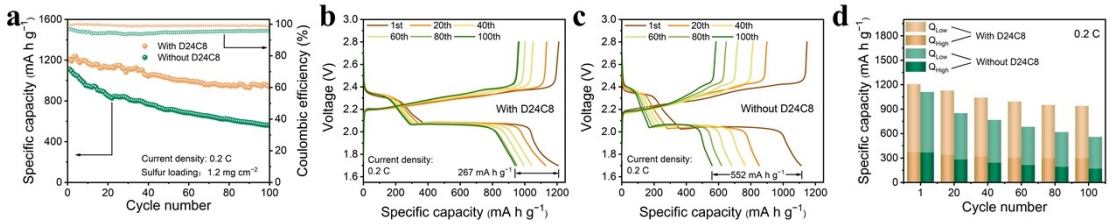

Figure S3. (a) Cycling stability of batteries with and without D24C8 at 0.2 C. Galvanostatic discharge-charge curves at different cycles of Li-S batteries (b) with and (c) without D24C8 at 0.2 C. (d) Stacked bar chart showing the discharge capacity distribution of Li-S batteries at different cycles in Q_{Low} and Q_{High}.

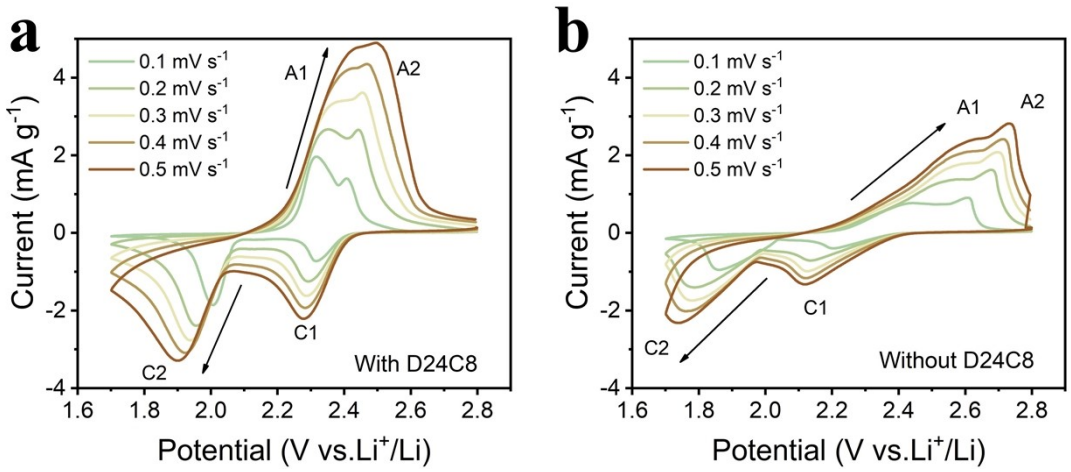

Figure S4. CV curves of the Li-S batteries (a) with and (b) without D24C8 at different scanning rate from 0.1 mV s^{-1} to 0.5 mV s^{-1}.

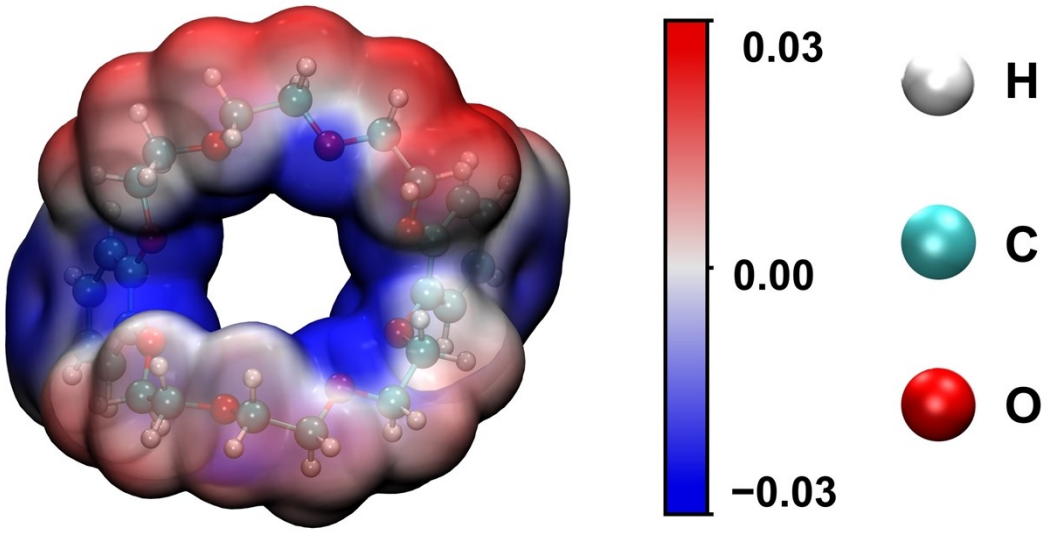

Figure S5. Electrostatic potentials (ESP) map of D24C8.

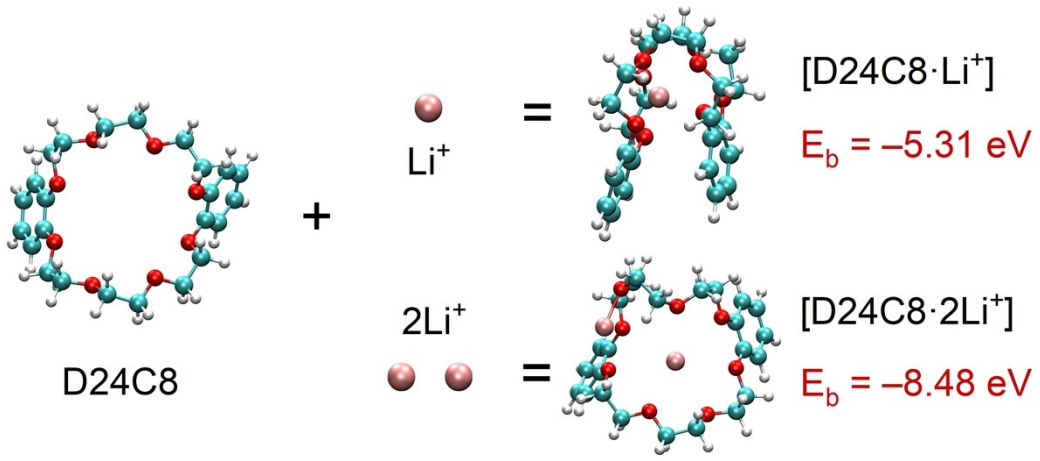

Figure S6. Optimised geometric structures and binding energies of D24C8 and D24C8 bonded Li^+ from DFT calculations. Eb is the binding energy between D24C8 and Li^+. The pink, red, blue and white balls denote the Li, O, C, and H atoms, respectively.

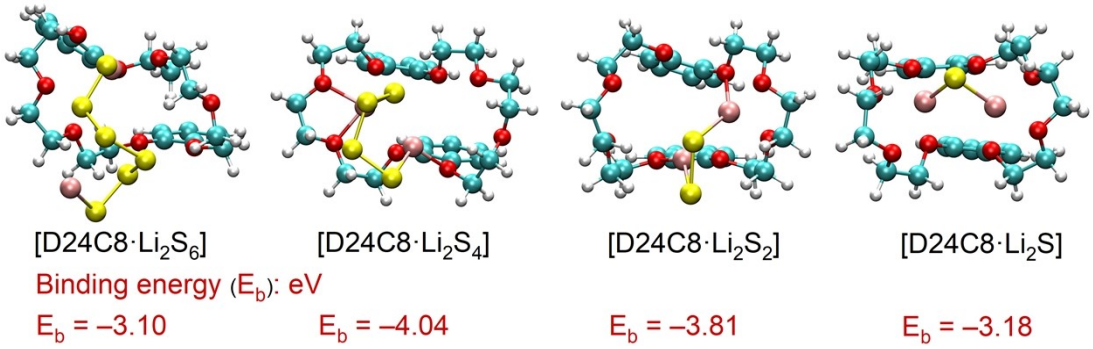

Figure S7. Optimised geometric structures and binding energies of D24C8 bonded Li^2S, Li^2S^2, Li^2S^4 and Li^2S^6 from DFT calculations. Eb is the binding energy between D24C8 and corresponding S species. The yellow, pink, red, blue and white balls denote the S, Li, O, C, and H atoms, respectively.

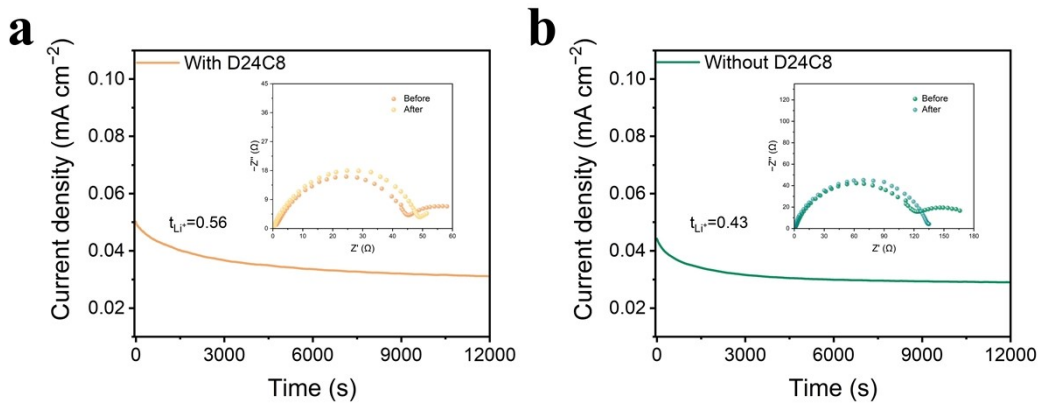

Figure S8. Chronoamperometry curves of batteies (a) with and (b) without D24C8. The corresponding EIS plots before and after polarization are shown in the inset.